Laponite immobilized TiO_2 catalysts for photocatalytic degradation of phenols

Erzsébet Décsiné Gombos[a], Dániel Krakkó[b], Gyula Záray[b], Ádám Illés[a], Sándor Dóbé[a], Ágnes Szegedi[a]*

[a]Research Centre for Natural Sciences, Hungarian Academy of Sciences, Institute of Materials and Environmental Chemistry, Budapest, 1117 Magyar tudósok krt. 2., Hungary

[b]Eötvös Loránd University, Institute of Chemistry, Department of Analytical Chemistry, Pázmány Péter sétány 1/A 1117, Budapest, Hungary

Corresponding author e-mail address: szegedi.agnes@ttk.mta.hu

Keywords: laponite, titania, photocatalysis, phenol, 2,4,6-trichlorophenol

Abstract

Laponite immobilized titania catalysts were prepared by a pillaring process and by hydrothermal synthesis (HT) applying different titania sources such as $TiCl_4$ and $TiOSO_4$. Textural investigations (XRD, TEM, N_2 physisorption) evidenced that by the pillaring procedure a high specific surface area (~450 m^2/g) mesoporous composite with 5-6 nm sized anatase nanoparticles were formed retaining the morphology of parent laponite structure. In contrast, by hydrothermal treatment with titanium oxysulfate the initial laponite structure was destroyed and a more opened nanoporous silica/titania material was formed with bigger, about 14 nm anatase particles.

FT-IR spectroscopic investigations revealed the different acidic character of titania/laponite composite samples showing stronger Lewis and weak Brönsted acid sites on both catalysts. However, acidic centers in titania pillared laponite stem from Ti–O–Si bonds, whereas in HT sample from the separated, ionic, surface sulfate species on titania.

Catalytic activity of titania/laponite composites were tested in photo-oxidation of model 10^{-5} M phenol and 2,4,6-trichlorophenol (TCP) water solutions. Catalytic tests were carried out in a home constructed batch-type photo-reactor with oxygen bubbling, and applying commercial low pressure Hg lamps emitting UV-light at 254 nm and 361 nm. Catalytic results showed that utilization of titania/laponite catalysts enhanced the photo-oxidation activity. Hydrothermally prepared sample showed much better catalytic performance than titanium chloride pillared one,

probably due to the bigger titania particles and the more opened mesoporous structure of titania/laponite HT, and moreover to the peculiar surface acidic properties of sulfated titania species. Separation of catalysts from reaction media even in tap water was much easier than that of commercial titania, i.e. by self-settling.

1. Introduction

Advanced oxidation processes (AOP) can be real solutions to conventional physical water treatment techniques for the removal of toxic and non-biodegradable organic pollutants, if they are quite efficient and cost effective [1, 2]. In industrial practice it seems that AOPs can be rather complementary methods to biological treatment, in order to reduce toxicity of effluents by converting the inherent pollutants to less harmful or biodegradable ones. Among AOPs photocatalytic degradation is one of the suitable alternatives. By assessment of performance and operating costs at pilot plant scale Ortega-Mendez et. al. [3] have found that by utilization of TiO_2 based photocatalysts, Evonik P 25, about 50 mg/L phenol containing waste waters can be treated economically. In heterogeneous AOPs, titania in the form of anatase appears to be the ultimate choice as photocatalyst for environmental applications. It has high photoactivity, stability under UV light and low price. From catalytic point of view, application of titania in an aqueous suspension would be more advantageous compared to its immobilization on a physical surface, however nanosized anatase powders have tendency to agglomerate into larger particles, more pronounced in tap water, and there are also difficulties in recovering it from the reaction media. Compared with the usual powdered photocatalysts, the easily recyclable photocatalysts have more advantages in water treatment and purification systems. Thus, immobilization of titania nanoparticles on a suitable support can overcome the above mentioned problems. Extensive research is in progress to find the appropriate, photo-chemically stable support, and plethora of sophisticated and more common substrates are tested [4]. Different types of porous silica [5] and clay mineral based titania composites attracted great interest due to the possibility to decrease the particle size of titania by dispersing it on high specific surface area supports and thus enhancing the oxidation potential of the catalysts. Titania can be incorporated into clay mineral structures by different ways. One of them is the so called pillaring procedure, when polymerized cations or positively charged nanoparticles are replacing the interlayer cations [6]. In this way amorphous or very small titania particles are formed between the clay mineral layers, showing poor photocatalytic activity [7]. Another approach is the synthesis of a porous composite structures, when a solid dispersion of crystalline anatase nanoparticles among the

swollen or decomposed silicate layer structure is formed, creating a more photoactive catalyst [7, 8]. The pore structure of the titania silica composite also plays a crucial role in the photocatalytic activity. TiO_2 pillared clays are microporous solids of moderate porosity [9], with less accessible active sites for the reactants. In contrast, composite materials with mesoporous structure and bigger crystalline titania nanoparticles can be optimal solution to meet the requirements of high photocatalytic activity and easier way of separation. From this point of view laponite, a crystalline, synthetic clay, isostructural with hectorite seems to be a particular and ideal candidate for the preparation of porous titania nanocomposites. It is well known that the special house of cards structure of laponite, creating exfoliated discrete plates of 20-30 nm in water suspension is more suitable for the synthesis of such composites than other smectite type clay minerals [9, 10]. Zhu et al. applied titanium hydrate sol as precursor, and found that aging at 100°C with laponite dispersion resulted in homogeneous deposition of metal hydrates on the acid-leached laponite layers [10]. During the aging period a reaction starts between the laponite crystallites and the acidic pillaring solution. The acid leached laponite layers suffer structural changes, meanwhile the high pH of laponite dispersion facilitates the formation of larger TiO_2 nanoparticles. Application of a surfactant can further enhance the porosity of the nanocomposite material. Applying the above concept Daniel et. al investigated the effect of synthesis parameters, such as pH, Ti/clay ratio, hydrothermal treatment and microwave heating [11, 12]. It was found that increased titania content and temperature of hydrothermal treatment, enhancing the crystallinity of anatase resulted in better performing photocatalysts. Australian scientists modified the above synthesis procedure by applying titanyl sulfate as titania source first on beidellite clay [13] than in the case of laponite [14]. They have found that by application of the acidic precursor and hydrothermal treatment, similar mesoporous composite structure was formed like with prehydrated titania sol, and that the catalytic activity could be enhanced by increasing the crystallite size of anatase and mesoporosity of the catalyst. Their TiO_2 immobilized clay mineral catalysts were comparably active in degradation of herbicides like P25 TiO_2 [15], but could be more easily separated from the reaction mixture.

Lin et. al. modified the titania/laponite catalysts with zirconia or ceria in order to achieve better photocatalytic performance [16]. Joo et al. have prepared active composite photocatalyst for the decomposition trichloroethylene by combining ZnO nanoparticles and PVA with laponite [17]. In this study, TiO_2/laponite nanocomposite materials were prepared by different methods (pillaring or hydrothermal treatment), applying different titania precursors in order to compare their photocatalytic activity in decomposition of model compounds such as phenol and 2,4,6-

trichlorophenol. $TiCl_4$ and $TiOSO_4$ were chosen as titanium precursors to avoid the application of titanium alkoxides, and to use low cost intermediates of TiO_2 white pigment manufacturing. Photocatalytic behavior was studied by the utilization of commercial low pressure Hg UV lamps of different wavelengths, to reveal the effect of different radiation energies. Textural and spectroscopic methods evidenced the structural peculiarities of the studied catalysts and made easier to interpret their distinct photocatalytic behavior.

2. Experimental section

2.1 Materials

The synthetic layered clay, laponite XLG grade was purchased from BYK-Chemie GmbH, Germany (formerly Rockwood Additives, now marketed by BYK Additives & Instruments). Titanium chloride, titanyl sulfate ($TiOSO_4 \cdot xH_2O$, 98%) hydrochloric acid and 2,4,6-trichlorophenol were obtained from Sigma-Aldrich. Phenol (>98%) was supplied by Loba Feinchemie GmbH. Commercial, fumed P25 TiO_2 was purchased from Evonik Industries AG, Germany.

2.2 Synthesis of TiO_2/Laponite catalysts

Laponite immobilized titania catalysts with different amounts of titania were prepared based on the procedure of Long et. al. [18, 19]. A solution of partially hydrolyzed Ti-polycations was prepared by adding $TiCl_4$ into a 2 M HCl solution. The mixture was than diluted by slowly adding deionized water with constant stirring to reach a final titanium concentration of 0.82 M. The final concentration of HCl was 0.6 M. The solution was aged for more than 8 h at room temperature prior to its use. Eight grams of laponite was dispersed in 2.0 L deionized water and the slurry was stirred for 5 h. The pillaring solution was slowly added into the suspension of clay with vigorous stirring until the amount reached 10 and 20 mmol Ti/g clay, respectively. The precipitated products were aged in the solution for 24 h. Subsequently, the clay particles were separated by centrifugation, and washed chloride free, evidenced by silver nitrate test. Samples were dried at 120°C for 12 h, and then calcined at 500°C for 12 h. The calcined samples containing different amounts of titania were designated as TiLapP1 and TiLapP2, respectively. Titania modified laponite was prepared also by the application of titanyl sulfate by the method of Yang et al. [14]. In a typical synthesis procedure 8 g of laponite was dispersed in 400 mL distilled water and vigorously stirred until clear, homogenous colloid solution was obtained. 25,6 g $TiOSO_4$ was dissolved by heating in 200 mL distilled water. 150 mL (15 mmol Ti/g

laponite) of the stock titanyl sulfate solution was added dropwise to the laponite suspension and stirred for 3 h. The mixture was transferred to a Teflon lined stainless steel autoclave, and kept under autogenous pressure at 150°C for 24 h. The solid precipitated by hydrothermal treatment was separated by centrifugation and washed neutral and sulfate free with distilled water. The sample was dried at ambient temperature. Then it was heat treated in a two-step procedure by 2°C/min heating rate first at 100°C for 1h and in the second step at 500°C for 3 h. The thus prepared sample was designated as TiLapHT.

The heat treated TiLap catalysts were grinded in agate mortar and the 0.08-0.02 mm grain size fraction, found to be easily separable from reaction media by settling, was tested in photocatalytic reactions.

2.3 Characterization

Chemical composition of the samples was determined by ICP-OES analysis (Spectro Genesis) after digesting the samples in cc. HF and sulfuric acid solution on a water bath.

X-ray powder diffraction patterns were recorded by a Philips PW 1810/3710 diffractometer with Bragg-Brentano para-focusing geometry applying monochromatized CuK_α (λ=0.15418 nm) radiation (40 kV, 35 mA) and proportional counter. For the identification of anatase phase ICDD PDF2 card No. 21-1272 was used. X-ray diffraction patterns were collected between 3 and 75°2θ with a 0.02°2θ step for 1 s.

Nitrogen physisorption measurements were carried out at -196°C using Thermo Scienctific Surfer automatic, volumetric adsorption analyzer. Before adsorption analysis, silica samples were outgassed under high vacuum ($<10^{-6}$ mbar) at 250°C for 2 h. Specific surface area was calculated by the BET equation between the 0.01-0.2 relative pressure. Pore size distribution was evaluated from the adsorption branch by the BJH method, as suggested by Rouquerol et al. [20].

TEM images were taken using a MORGAGNI 268D transmission electron microscope (100 kV; W filament; point-resolution = 0.5 nm). Samples were suspended in a small amount of ethanol and a drop of suspension was deposited onto a copper grid covered by carbon supporting film and dried at ambient.

Diffuse reflectance spectra in the UV-Vis region were detected at ambient by a Jasco V-670 UV-Vis spectrophotometer equipped with NV-470 type integrating sphere using the official $BaSO_4$ standard as reference.

Ammonia ion exchange capacity of the parent laponite and its titania modified varieties were determined by contacting 1 g clay with 25 ml 1 M ammonium chloride solution for 3h. The

procedure was repeated two more times by fresh ammonia solution after separation with centrifugation. After the third mixing, the clay was centrifuged and washed with distilled water until chloride free and dried at ambient temperature. Ammonia concentration was determined by temperature programmed desorption of ammonia by heating the sample with 10°C/min rate to 600°C in a sealed glass reactor in N_2 stream, and automatically titrating the evolved ammonia absorbed in distilled water by 0.1 M hydrochloric acid.

FT-IR spectroscopic measurements were carried out by a Nicolet Compact 400 spectrophotometer equipped with a special measuring cell with in situ pretreatment facility in high vacuum ($5 \cdot 10^{-6}$ mbar). Applying the self-supported wafer technique spectra of 100°C adsorbed pyridine (Py=7 mbar), desorbed in high vacuum at different temperatures (100-200-300-400°C) were obtained. Before Py adsorption catalyst wafers were dehydrated at 300°C in high vacuum. The spectra were normalized to 5 mg/cm^2 "thickness" for comparison.

2.4 Photocatalytic experiments

A self-constructed, batch-type cylindrical photochemical glass reactor was used with internal diameter and overall length of 70 x 480 mm. The irradiating lamp was positioned coaxially in a quartz tube, in the center of the cylindrical reactor and was cooled by nitrogen flow to avoid the overheating of the lamp and keeping the reaction temperature constant, close to ambient at 32 ± 4 °C. Volume of the reaction mixture was 650 cm^3, which contained the model compounds, phenol or 2,4,6-trichloro phenol (TCP), dissolved in distilled water and the photocatalyst suspended by sonication prior to irradiation. The concentration of phenol or TCP was $5 \cdot 10^{-5}$ M, whereas that of the catalyst was 0.1–0.4 g/L. Pure oxygen was used for photooxidation that was fed into the reactor from the bottom through a fritted glass filter with 900 cm^3/min flow rate; the intensive bubbling served also as an efficient stirring of the catalyst slurry. Before starting the reaction, the catalyst suspension was equilibrated with oxygen for 10 minutes without switching the lamp on. One of the objectives of our study was to test the photocatalytic applicability of commercially available low pressure Hg lamps manufactured by LighTech Lamp Technology Ltd., Hungary. Therefore, two types of custom lamps with measures of 15 mm outer diameter x 360 mm length were used. One of them was the GHO436T5L type, "low ozone generating", germicidal lamp irradiating in the UV-C region at 254 nm with 13 W UV-radiant. The other one was a GHO245T6L/4-UVA type lamp irradiating in the 316-400 nm range with 4.6 W UV power, with the maximum at 361 nm. During the photocatalytic tests at certain intervals 5 cm^3 sample was taken of the reaction mixture, filtered with 45 μm Millipore filter and analyzed using Agilent Technologies 1200 series HPLC apparatus equipped with a

UV detector and a Phenomex Luna (5 μm, 250x4.6 mm) type reversed C18 column. The mobile phase was acetonitrile/water in the ratio of 30:70 and 60:40 for the determination of phenol and TCP conversion, respectively. The flow rate was 1.5 mL/s. Signal of phenol was detected at 270 nm, and that of TCP at 280 nm. Concentration depletion of phenol and TCP was calculated by the plotting of calibrated HPLC peak areas against the irradiation time.

In comparison, degradation of phenol and TCP were also investigated by photooxidation, i.e. without application of catalysts. Photocatalytic activities of the prepared TiO_2/laponite samples were also compared to that of commercial TiO_2, P25. The applied amount of P25 catalyst corresponded to the titania content of the titania/laponite composite samples.

3. Results and discussion

3.1 Textural characterization

Textural properties of the prepared different types of laponite immobilized titania catalyst were characterized by X-ray powder diffraction, and nitrogen physisorption. The XRPD patterns and nitrogen adsorption isotherms are shown in Fig 1 and 2, respectively. Chemical composition and textural characteristics are summarized in Table 1. XRD pattern of parent synthetic laponite clay, showing the widened reflections typical for disordered hectorite structure, can be indexed according to reference [21], with a $d_{(001)}$ peak corresponding to 1.1 nm. All the titania containing samples show only the presence of crystalline anatase phase. However, the average crystallite size calculated by the Sherrer equation differ significantly (Table 1). Samples modified with pillaring $TiCl_4$ solution show widened anatase reflection in connection with the small crystallite size, around 6 nm. The calculated average titania crystallite size of TiO_2/Lap HT sample is somewhat bigger, ~ 12 nm, whereas this value for P25 titania is amounted to 35 nm (Table 1). Some weak reflections of laponite (e.g. 110) remained after pillaring process, however by titanyl sulfate modification reflections of laponite cannot be observed any more. The increase of background between 20-30°2θ of TiO_2/LapHT sample can be associated with the formation of amorphous silica. The latter indicates the deterioration of parent laponite structure by acidic dissolution of sodium, magnesium and lithium cations resulting in layer degradation and framework collapse [14].

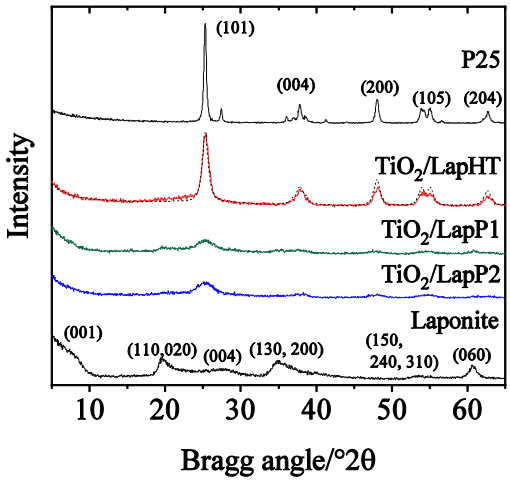

Fig. 1 X-ray powder diffraction patterns of the parent laponite and its TiO_2 modified varieties compared to commercial P25. Dashed curve for TiO_2/LapHT sample represents the pattern calculated by profile fitting method for the crystallite size determination of anatase.

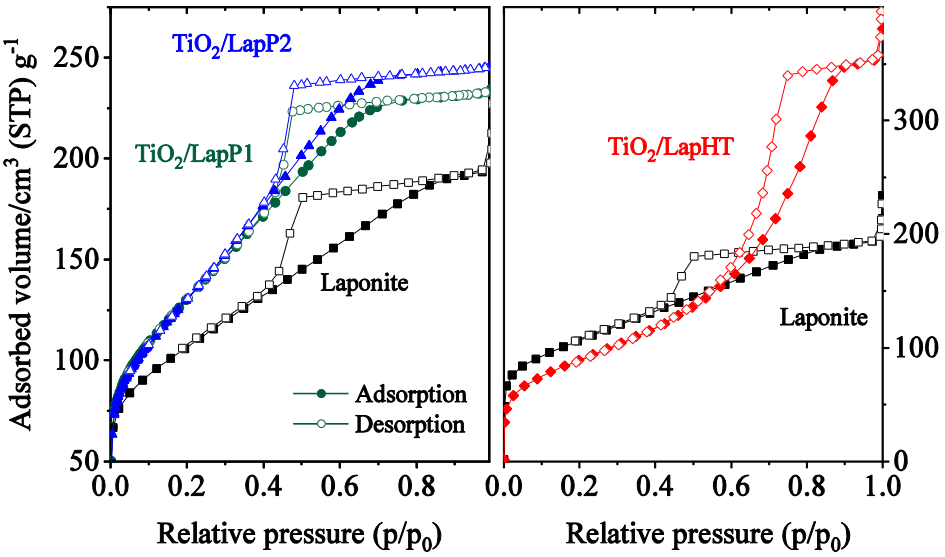

Fig. 2 N_2 physisorption isotherms of the studied TiO_2/Laponie samples compared to parent laponite

Nitrogen physisorption results support the above-mentioned observations (Fig. 2). Parent laponite and the titania modified samples TiO_2/LapP1-2 exhibit type IV(a) isotherms, [20] with H2 hysteresis loop, and a long, flat plateau, characteristic for materials with not ordered, 'complex pore structure made up of interconnected networks of pores of different size and shape' [20], in this case probably mainly slit-shaped ones. Increased specific surface area and pore volume are observed for samples modified by $TiCl_4$. This can be due to the partial

delamination of the house-of-card structure of laponite by the titania nanoparticles resulting in a more opened structure with somewhat bigger pores. Pore size analysis assessed by BJH method from the adsorption branch has indeed revealed a 10% increase in pore diameter from 3 to 3.3 nm. TiO_2/LapHT sample made by titanyl sulphate modification showed a quite different nitrogen physisorption isotherm. The adsorbed volume significantly increased and the hysteresis loop of IV type isotherm became a transitional one between H1 and H2 types. The specific surface area slightly decreased due to the much bigger pores (~7.5 nm), but the pore volume doubled (Table 1). This observation implies the total deterioration of the parent laponite structure and the formation of a titania-silica composite material [14, 15]. The bigger pores of the composite material arise from the interparticle voids.

Chemical composition analysis of the parent laponite and the titania modified samples support the above conclusions. Sodium content of all the titania containing samples significantly decreased, but leaching of magnesium was partial for P1 and P2 samples and complete for HT one (Table 1). Interestingly, ion-exchange capacity of P1-P2 samples increased to 3 times higher value, indicating that the platelets of laponite are detached from each other but remained more or less intact. This alteration of ion-exchange capacity can be useful by further modification of samples with other cations, e.g. transition metals. Titania content of TiLApP1 and TiLapHT samples are similar around 6.5 mmol/g, whereas TiLapP2 sample showed only a 10 % higher value, 7.5 mmol/g. There is no use to put higher amount of titania precursor to the synthesis mixture, the maximal amount of titania to be incorporated seems to be about 30–35 wt.%.

TEM investigation of the prepared catalysts support the results of other textural methods. TEM images are shown in Fig. 3. Parent laponite shows the well-known lamellar structure of laponite platelets with thickness of ~ 1 nm. By modification with the pillaring $TiCl_4$ solution small and poorly crystallized titania nanoparticles among the clay sheets can be observed, in accordance with XRD results.

By the hydrothermal treatment of titanyl sulfate containing laponite suspension, total transformation of the clay mineral is achieved and 10-15 nm sized, evenly dispersed, spherical titania and silica particles are formed. TEM investigations support the nitrogen physisorption data, i.e. enhanced porosity of the TiO_2/LapHt sample is due to inter-crystallite cavities. Titania nanoparticles are homogeneously dispersed among the silica particles. The titania/silica ratio influences the hydrophobicity of the sample, since silica nanoparticles are covered by silanol groups.

Table 1 Textural properties of the studied samples

Sample	S_{BET} m^2/g	PD[1] nm	TPV cm^3/g	Na mmol/g	Mg mmol/g	Ti mmol/g	NH_3 IEC[2] mmol/g	TiO_2 cryst. size[3] nm
Laponite	375	3.0	0.278	1.6	4.7	-	0.22	-
TiO_2/LapP1	447	3.33	0.377	0.02	1.7	6.7	0.79	5.3
TiO_2/LapP2	450	3.35	0.359	0.02	0.8	7.5	0.65	5.9
TiO_2/LapHT	323	7.45	0.542	0.02	0.02	6.8	0	12
P25	50	-		-	-	12.5	-	35

[1] Pore diameter determined by BJH method from the desorption branch of the isotherm

[2] Determined by ammonia TPD method following ammonium chloride ion-exchange procedure

[3] Determined by XRPD based on Sherrer equation and profile fitting method

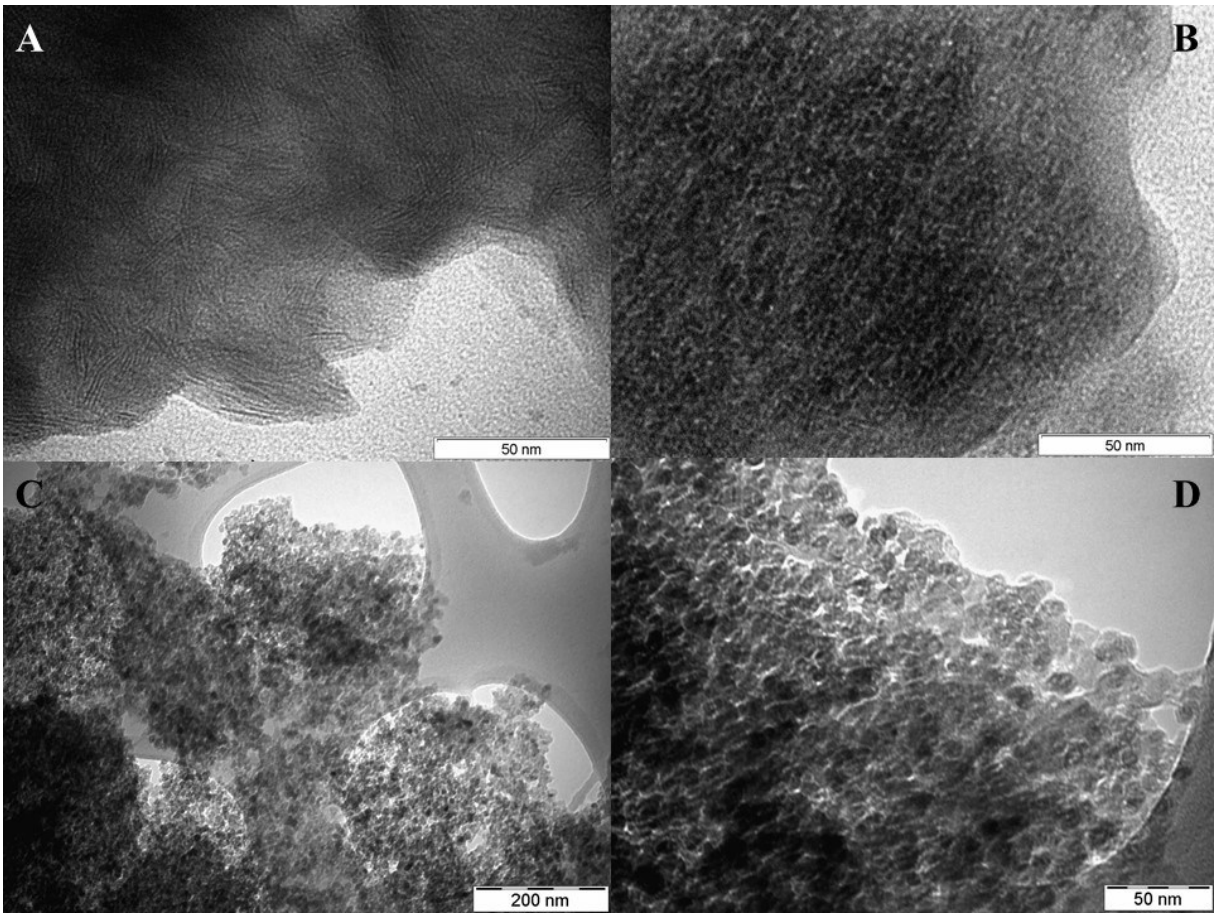

Fig. 3 TEM images of the parent laponite and laponite immobilized titania varieties: Laponite (A), TiO_2/LapP2 (B), TiO_2/LapHT (C, D)

Macroscopic properties of the laponite based catalysts, important from the separation point of view, were also characterized by scanning electron microscopy (Supporting info, Fig. S1, S2). Laponite supported titania catalyst show the picture of a grinded mineral, i.e. several μm sized, irregularly shaped, angular particles with very wide particle size distribution. By bigger magnification the layered structure of laponite can be clearly visualized by TiLapP2 sample. SEM images revealed that the morphology is quite different from that of P25 titania, the latter consisting of 35-50 nm sized nanoparticles.

Separation properties of the different catalyst were evaluated by measuring their settling velocity. The method of determination and the results are summarized in Supporting information in Fig S4-5 and Table 2. The result show that the laponite immobilized titania catalysts have similar but two orders of magnitude higher settling velocity than P25 titania. It is not surprising according to the very different morphology of the two types of catalysts evidenced also by SEM images.

3.2 Spectroscopic investigations: UV-Vis and FT-IR spectrophotometry

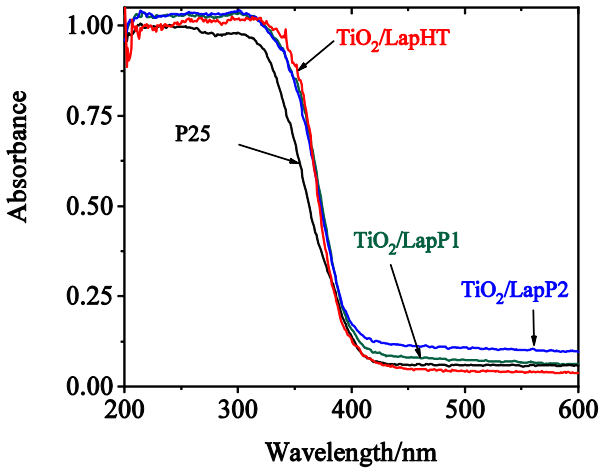

Fig. 4 DR UV-Vis spectra of the prepared laponite immobilized titania samples compared to commercial P25 titania

The band gap energy of titania can be investigated by the help of DR UV-Vis spectroscopy. The DR UV-Vis spectra of the prepared catalysts compared to commercial P25 are shown in Fig. 4. The characteristic absorption band of anatase can be found at 330 nm, corresponding to 3.2 eV band gap energy. Finely dispersed anatase phase regularly shows blue-shifted absorption band due to quantum size effect of nanoscaled particles or interface interactions [22]. In our case no band shift of the prepared catalysts to lower wavelength can be observed, however the

slope of absorption edge slightly increased, indicating a negligibly higher band gap energy for the laponite-immobilized titania samples. Spectra of samples prepared by the different methods are very similar to each other. DR UV-Vis spectra evidence that our catalysts can be photocatalytically active when illuminated by UV-A, or shorter wavelength light, but similarly to P25 they are not in the visible region.

When silica materials are modified with titania, Ti–O–Si bonds can be formed between the silica-titania interface [23]. When titania is incorporated into a silica matrix Lewis and Brönsted acid surface sites are generated [23]. One can get information about the amount and nature of acidity of catalysts by adsorption of a base on them and investigating the formed surface species by FT-IR spectroscopy. Pyridine (Py) is a well-known and verified adsorbent for the characterization of acid sites of metal oxides, zeolites etc. The 8a, 8b and 19b ring vibrations (ν_{CCN}) of Py give adsorption bands in the 1700-1400 cm^{-1} frequency region. Py can be physisorbed or H-bonded to silanol groups (H-Py), coordinated to Lewis acid sites (L-Py) or

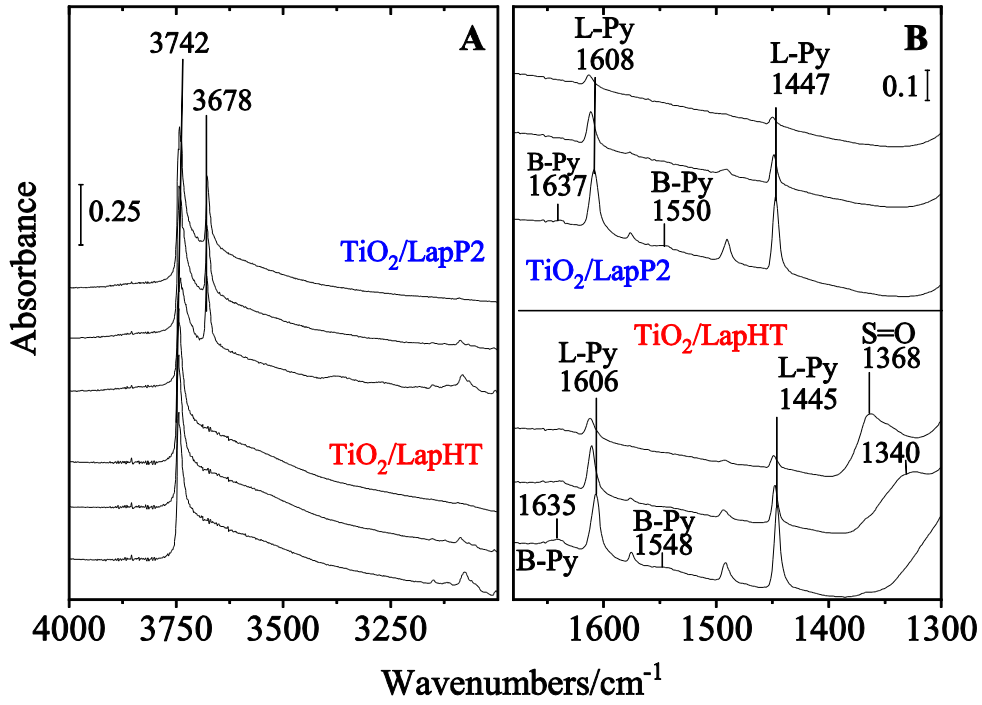

Fig. 5 FT-IR spectra of adsorbed Py on titania modified laponite samples. Py was adsorbed on 300°C dehydrated samples at 100°C, and desorbed at 100-200-300°C (from bottom up)

protonated on Brönsted acid centers (B-Py). The latter one gives a band at 1545 cm^{-1}, whereas H-Py bands appear at 1446 and 1598 cm^{-1}, and L-Py bands at 1448 and 1610 cm^{-1} frequencies.

The FT-IR spectra of pyridine adsorbed on the studied titania modified samples are shown in Fig. 5 A and B. It can be observed that on both types of samples relatively higher concentration of Lewis acid sites can be found compared to that of Brönsted type. These sites can be formed when titania is interacting with the silica framework, and Ti–O–Si bonds are formed [23]. Ti–O–Si bridges can generate Brönsted acid sites when Ti atoms are in octahedral coordination and hydroxyl groups or water molecules are in the vicinity of their coordination spheres. In the absence of coordinated water or hydroxyl groups incorporated Ti species behave as Lewis acid centers. The intensity of L-Py bands is related to the concentration of the Ti–O–Si bonds available for Py molecules to be adsorbed. According to FT-IR spectra there is no significant difference between acidic character of the titania/laponite samples prepared by the two different methods, and it seems that only a small amount of Ti is involved in the Ti–O–Si bond formation reaction. The strength of acid sites can be characterized by the desorption temperature of pyridine. Py is mainly desorbed from the Brönsted centers even at 200°C, demonstrating very weak acidity of the samples. Lewis acid centers show higher acid strength, Py can be desorbed totally from these centers only at 400°C. On the other hand, the acidity of TiLapHT sample originates rather from surface sulfate groups and not from Ti–O–Si bond formation, as evidenced by the presence of S=O stretching vibration band at 1368 cm^{-1}. Sulfate groups can probably be localized on the surface of bigger titania particles, and their formation can be due to the reaction of sulfuric acid originating from decomposition of titanium oxysulfate with the titania nanoparticles during the hydrothermal treatment. Formation of covalent disulfate species is hindered by the size of titania nanoparticles (~ 12 nm). According to Barthos and Lónyi et al. [24, 25] the S=O stretching vibration band found between 1340-1385 cm^{-1} is characteristic of isolated, monosulfate groups with ionic character. S=O stretching vibration band characteristic for covalently bond disulfate species appear around 1400 cm^{-1} [25]. Liu et al. [26] have found the S=O band appearing at 1390 cm^{-1} on sulfated bulk titania photocatalyst with higher sulfur content. Upon Py adsorption, the S=O bands totally disappear, which support the idea that they are located on the surface of titania, and do not belong to unreacted titania oxysulfate or titania sulfate species. Upon desorption of Py at 200 °C the band appear somewhat redshifted to 1340 cm^{-1}, then totally restored at 300°C (fig. 5). This phenomenon is well known on sulfated titania/titania-zirconia/silica catalyst [25]. The chemisorbed pyridine can backdonate electrons to the sulfate groups through the titanum ion, changing its character to more ionic. This change induces the shift of the $\nu_{S=O}$ band to lower frequencies.

Detection of surface sulfate species on TiLapHT sample means that this catalyst has titania species not only differing in size but also in acidity and surface properties compared to that of titanium chloride pillared ones.

The different surface characteristic of the two laponite-titania composites was also supported by the FT-IR spectra in the OH region (Fig. 5A). TiLApHT sample show typical OH bands characteristic for amorphous silica. The intensive band at 3742 cm^{-1} is associated with terminal silanol groups and the wide band around 3600 cm^{-1} belongs to hydrogen bonded neighboring silanols. In the spectra of TiLapP2 sample a band at 3678 cm^{-1} also appears. The latter is characteristic for the Mg-OH vibration. This observation is in line with our former chemical analysis and textural characterization results, indicating that the parent laponite structure was still preserved.

3.3 *Photocatalytic activity*

Photocatalytic activity of the synthesized titania/laponite composite catalysts was tested by studying the degradation of model compounds, phenol and 2,4,6-trichloro phenol (TCP) in water solution. Two types of commercially available low pressure Hg lamps were applied, providing UVC and UVA radiation at 254 nm and 361 nm, respectively. Fig. 6 shows the results obtained by UVC irradiation of phenolic solution, containing $5 \cdot 10^{-5}$ M phenol. Photocatalytic oxidation efficiencies of TiO_2/lap catalysts were compared to that of commercial P25 titania and to photooxidation without added catalyst. The amount of P25 was chosen to contain equal amount of titania with that of TiO_2/Lap samples (see Table 1). It is observed that TiO_2/LapHT sample degrades phenol in 20 minutes, showing superior activity compared to TiO_2/LapP2 catalyst and photooxidation (Fig. 6). P25 exhibit somewhat better performance eliminating phenol within 10 min. Decomposition of TCP was very fast on all catalysts and also by photooxidation by using UVC irradiation, it was completed within 5 minutes.

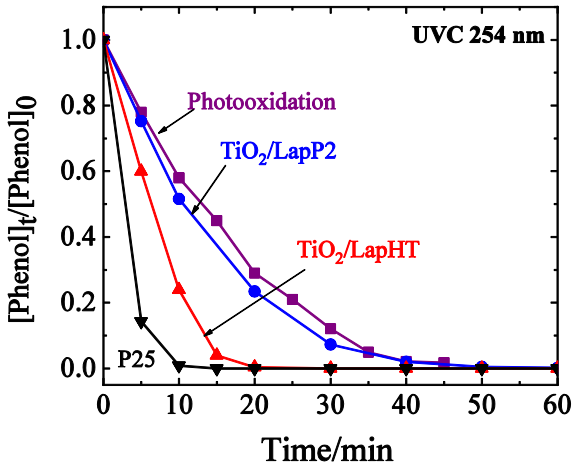

Fig. 6 Degradation of phenol by photo-, or photocatalytic oxidation with 254 nm UVC irradiation on titania/laponite catalysts compared to commercial P25 titania

It seems that reaction rate of TCP oxidation is higher and activation energy is much lower than that of phenol under similar reaction conditions. It is well known phenomena from photodegradation studies of phenol and chlorophenols, that substitution pattern of phenol strongly influences the rate of photodegradation [27]. Thus, most probably, adsorption properties of different phenols on the hydrophilic surface of titania composite, and the complex equilibrium conditions of the three adsorbed phases (oxygen, phenol/TCP, titania/silica) are responsible for the different photocatalytic behavior.

In order to more closely study the effect of catalysts rather than that of high energy irradiation, the photodegradation of phenol and TCP was investigated also by UVA irradiation, with lower energy input. The determined depletion data are presented in Fig. 7. Trends, similar to those experienced with UVC radiation were observed for the catalytic activity. Application of titania/laponite composites significantly increased the reaction rate compared to simple photooxidation, and TiO_2/LapHT sample showed better catalytic performance than the pillared variety, TiO_2/LapP2. Commercial P25 titania exhibited similarly high activity like before, degrading phenol in 15 min.

Decomposition of TCP was also faster with the applied catalysts than that of phenol, but total decomposition could be only achieved with P25 and TiO_2/LapHT catalyst, in 15 and 80 min, respectively. As expected, the catalytic acceleration has been found more apparent at the longer wavelength of 361 nm compared to 254 nm. Referenced to non-catalyzed photooxidation, phenol depletes ~2 times and ~15 times faster in photocatalytic oxidation with TiO_2/LapHT and P25 catalysts, respectively. Similarly, the rate enhancing effect for TCP is a factor of 4 and 18 using the above catalysts.

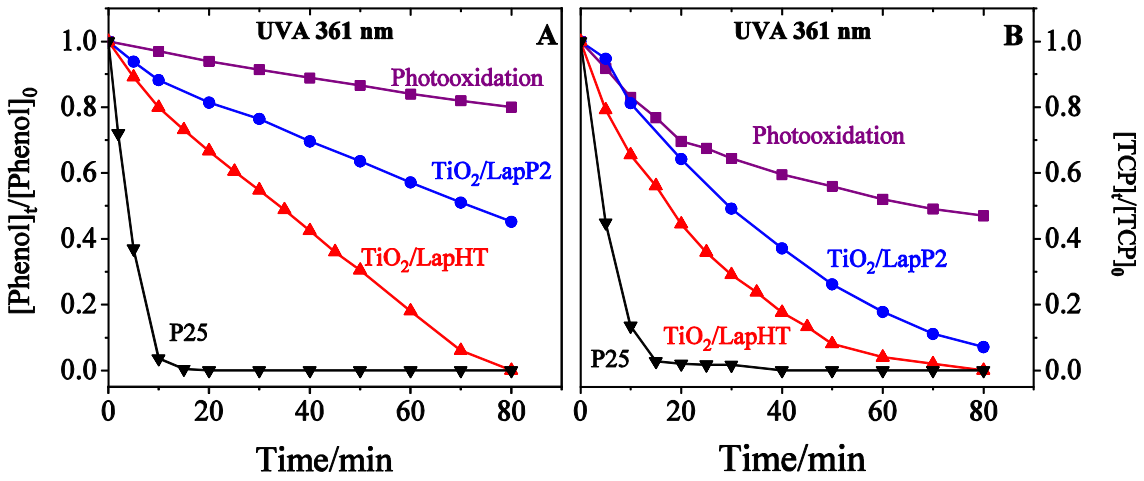

Fig. 7 Degradation of phenol (A) and 2,4,6-trichloro phenol (B) by photo-, or photocatalytic oxidation with 361 nm UVA irradiation on titania/laponite catalysts compared to commercial P25 titania

This is in line with the observation, that the homogeneous depleting process of direct photolysis and OH radical reactions play a decreasing role with increasing wavelength, and heterogeneous surface reactions become more dominant. The fact that phenol and TCP undergo photooxidation in the absence of a catalyst at 361 nm is surprising, since these molecules does not absorb light at this relatively long wavelength. One possible explanation has recently been provided in conjunction with the thermal oxidation of chlorophenols, where the accelerating effect of stray light was attributed to the formation of quinones, photocatalytically active intermediates in the reaction [28, 29].

In summary, it was found that titania/laponite composite material prepared by titanium oxysulfate and hydrothermal method was more active in decomposition of phenol and TCP than titania/laponite pillared catalyst, but could not exceed the activity of commercial P25 titania. The significant difference in catalytic activity of the two titania/laponite composites can be explained by their structural characteristics. TiO_2/LapHT catalyst can be considered rather a mesoporous mixed oxide composite material possessing well-crystallized, bigger anatase nanoparticles that can be easily accessed by the reactant molecules. For porous structures, the diffusion of reactant molecules can be a rate-determining step: smaller pore size can hinder the diffusion. TiO_2/LapP catalysts have bigger surface area because of its much smaller pore size, and very small anatase particles that are confined in the laponite structure. The peculiar pore structure and the optimal crystallinity of anatase nanoparticles seem to have beneficial effect on photocatalytic activity in TiO_2/LapHT. Similar trends were found by B. Paul et.al. [15]

investigating herbicide decomposition on titania/laponite composite materials. Surface charge, hydrophobic-hydrophilic character of the catalyst can also influence the catalytic activity by favoring the adsorption of reactant molecules on active surface species. From this point of view, it seems that both types of titania/laponite composite have weak Brönsted and Lewis acidic character as a consequence of Ti–O–Si bond formation during the synthesis, or due to the presence of isolated sulfate groups on the surface of titania nanoparticles as it is the case concerning TiO_2/LapHT sample. However, the presence of surface sulfate groups on TiLapHT sample and the Mg-OH groups in TiLapP samples can significantly affect the electron structure of anatase particles. Liu et. al. [26] have found that ionic sulfate species, with S=O bond order less than two, representing coordinatively unsaturated Lewis acid sites have beneficial effect on photocatalytic activity. Surface sulfate species can withdraw electrons from the neighboring Ti^{4+} cations, resulting in increased electron deficiency. The presence of acid sites can improve the charge separation of the photo-generated electrons and holes and hinder the recombination of electron-hole pairs. In contrast, high sulfate coverage of titania and formation of covalent disulfate species rather reduce the photocatalytic activity.

In order to find some correlation between the surface properties and photocatalytic activity, liquid phase adsorption of phenol on the studied catalysts was investigated. Results are summarized in Supporting information Fig S3, and table S1. Our experiments revealed that by the applied photocatalytic reaction parameters, it is not possible to reach the equilibrium concentration, and the dispersion of the catalysts, especially in the case of P25 plays important role in the adsorbed amount of phenol. Our adsorption experiments clearly evidenced that P25 titania adsorbs at least two times higher amount of phenol than the laponite immobilized ones. This can be one reason, among the many other factors, influencing the catalytic activity. The adsorption behavior by one-hour contact time show similar tendency like the photocatalytic activity, being P25 the most active one, followed by TiLapHT sample. By 24 h adsorption the adsorbed amount of phenol significantly increased, but P25 still overcomes the laponite supported titania catalysts.

Titania/laponite composite catalysts have been found to be inferior in photatalytic activity compared to commercial titania. They do have, however showed the practical benefit, that they can be easily recovered from the reaction slurry by settling or filtration. As evidenced also by our investigations, the sedimentation rate of P25 catalyst is very slow, it needs several hours to be settled.

Conclusions

Our experiments have proved that laponite is a suitable support for the production of easily separable TiO_2-based catalysts. Applying different titania immobilization procedures, it turned out that although 'pillaring' process opens the laponite structure, only 5-6 nm TiO_2 nanoparticles are incorporated in between the layers. By applying hydrothermal treatment and acidic $TiOSO_4$ precursor, the laponite structure is converted to a silica/titania nanocomposite with 12-14 nm titania particles. FT-IR study of adsorbed pyridine revealed the different acidic character of the studied catalysts, evidencing the presence of sulfate species on the surface of titania phase in TiO_2/LapHT sample. The latter catalyst is more active in photocatalytic degradation of phenol and 2,4,6-trichlorophenol than the 'pillared' one, probably due to bigger size of crystalline titania nanoparticles, to the peculiar pore system and different acidity. It was also found that P25 titania overcomes the catalytic activity of laponite based titania catalysts but it has the drawback that can hardly be separated from the reaction media by sedimentation or filtration.

Acknowledgements

Financial support of the National Research, Development and Innovation Office of Hungary (NKFIH, NVKP_16-2016-1-0045, 'Innovative photooxidation water cleaning technology') is greatly acknowledged. The authors thank to Dr. Zoltán Dankházi, at the Eötvös Loránd University, Faculty of Science, SEM/FIB laboratory, for the scanning electron microscopic images.

Figure captions

Fig 1. X-ray powder diffraction patterns of the parent laponite and its TiO_2 modified varieties compared to commercial P25. Dashed curve on TiO_2/LapHT sample represents the pattern calculated by profile fitting method for the crystallite size determination of anatase.

Fig. 2 N_2 physisorption isotherms of the studied TiO_2/laponite samples compared to parent laponite

Fig. 3 TEM images of the parent laponite and laponite immobilized titania varieties: Laponite (A), TiO_2/LapP2 (B), TiO_2/LapHT (C, D)

Fig. 4 DR UV-Vis spectra of the prepared laponite immobilized titania samples compared to commercial P25 titania

Fig. 5 FT-IR spectra of adsorbed Py on titania modified laponite samples. Py was adsorbed on 300°C dehydrated samples at 100°C, and desorbed at 100-200-300°C (from bottom up)

Fig. 6 Degradation of phenol by photo-, or photocatalytic oxidation with 254 nm UVC irradiation on titania/laponite catalysts compared to commercial P25 titania

Fig. 7 Degradation of phenol (A) and 2,4,6-trichlorophenol (B) by photo-, or photocatalytic oxidation with 361 nm UVA irradiation on titania/laponite catalysts compared to commercial P25 titania

References

[1] M. Pera-Titus, V. García-Molina, M.A. Baños, J. Giménez, S. Esplugas, Degradation of chlorophenols by means of advanced oxidation processes: A general review, Appl. Catal. B Environ. 47 (2004) 219–256. doi:10.1016/j.apcatb.2003.09.010.

[2] S. Sharma, M. Mukhopadhyay, Z.V.P. Murthy, Treatment of chlorophenols from wastewaters by advanced oxidation processes, Sep. Purif. Rev. 42 (2013) 263–295. doi:10.1080/15422119.2012.669804.

[3] J.A. Ortega-Méndez, J.A. Herrera-Melián, J. Araña, M.R. Espino-Estévez, J.M. Doña-Rodríguez, Performance and Economic Assessment of the Treatment of Phenol with TiO_2 Photocatalysis, Photo-Fenton, Biological Aerated Filter, and Wetland Reactors, Chem. Eng. Technol. 40 (2017) 1165–1175. doi:10.1002/ceat.201600159.

[4] B. Srikanth, R. Goutham, R. Badri Narayan, A. Ramprasath, K.P. Gopinath, A.R. Sankaranarayanan, Recent advancements in supporting materials for immobilised photocatalytic applications in waste water treatment, J. Environ. Manage. 200 (2017) 60–78. doi:10.1016/j.jenvman.2017.05.063.

[5] R. Peng, O. Ridge, Removal of Hazardous Pollutants from Wastewaters : Applications of TiO_2-SiO_2 Mixed Oxide Materials Removal of Hazardous Pollutants from Wastewaters : Applications of TiO_2 -SiO_2 Mixed Oxide Materials, 2014 (2016). doi:10.1155/2014/617405.

[6] B. Szczepanik, Photocatalytic degradation of organic contaminants over clay-TiO_2 nanocomposites: A review, Appl. Clay Sci. 141 (2017) 227–239. doi:10.1016/j.clay.2017.02.029.

[7] T. Albanis, P. Pomonis, I. Konstantinou, D. Petridis, A. Katsoulidis, D. Lambropoulou, V. Belessi, Structure and photocatalytic performance of TiO2/clay nanocomposites for the degradation of dimethachlor, Appl. Catal. B Environ. 73 (2006) 292–299. doi:10.1016/j.apcatb.2006.12.011.

[8] A. Mishra, A. Mehta, M. Sharma, S. Basu, Enhanced heterogeneous photodegradation of VOC and dye using microwave synthesized TiO_2/Clay nanocomposites: A comparison study of different type of clays, J. Alloys Compd. 694 (2017) 574–580. doi:10.1016/j.jallcom.2016.10.036.

[9] H.Y. Zhu, J.A. Orthman, J.Y. Li, J.C. Zhao, G.J. Churchman, E.F. Vansant, Novel composites of TiO2(anatase) and silicate nanoparticles, Chem. Mater. 14 (2002) 5037–5044. doi:10.1021/cm0205884.

[10] H.Y. Zhu, J.C. Zhao, J.W. Liu, X.Z. Yang, Y.N. Shen, General synthesis of a mesoporous composite of metal oxide and silicate nanoparticles from a metal salt and Laponite suspension for catalysis, Chem. Mater. 18 (2006) 3993–4001. doi:10.1021/cm060390+.

[11] L.M. Daniel, R.L. Frost, H.Y. Zhu, Synthesis and characterisation of clay-supported titania photocatalysts, J. Colloid Interface Sci. 316 (2007) 72–79. doi:10.1016/j.jcis.2007.08.023.

[12] L.M. Daniel, R.L. Frost, H.Y. Zhu, Laponite-supported titania photocatalysts, J. Colloid Interface Sci. 322 (2008) 190–195. doi:10.1016/j.jcis.2008.02.029.

[13] Z. Yuan, H. Zhu, X. Gao, Y. Shen, R.L. Frost, W.N. Martens, J. Liu, X. Yang, A mesoporous structure for efficient photocatalysts: Anatase nanocrystals attached to leached clay layers, Microporous Mesoporous Mater. 112 (2007) 32–44. doi:10.1016/j.micromeso.2007.09.017.

[14] Y. Xuzhuang, D. Yang, Z. Huaiyong, L. Jiangwen, W.N. Martins, R. Frost, L. Daniel, S. Yuenian, Mesoporous structure with size controllable anatase attached on silicate layers for efficient photocatalysis, J. Phys. Chem. C. 113 (2009) 8243–8248. doi:10.1021/jp900622k.

[15] B. Paul, W.N. Martens, R.L. Frost, Immobilised anatase on clay mineral particles as a photocatalyst for herbicides degradation, Appl. Clay Sci. 57 (2012) 49–54. doi:10.1016/j.clay.2011.12.009.

[16] Y. Lin, P. Pi, Z. Yang, L. Wang, Synthesis and photocatalytic property of the ZrO_2/TiO_2 pillared laponite, J. Wuhan Univ. Technol. Mater. Sci. Ed. 26 (2011) 852–856. doi:10.1007/s11595-011-0324-z.

[17] J.C. Joo, C.H. Ahn, D.G. Jang, Y.H. Yoon, J.K. Kim, L. Campos, H. Ahn, Photocatalytic degradation of trichloroethylene in aqueous phase using nano-ZNO/Laponite composites, J. Hazard. Mater. 263 (2013) 569–574. doi:10.1016/j.jhazmat.2013.10.017.

[18] R.Q. Long, R.T. Yang, Selective Catalytic Reduction of Nitrogen Oxides by Ammonia over Fe^{3+}-Exchanged TiO_2-Pillared Clay Catalysts, J. Catal. 268 (1999) 254–268. doi:10.1006/jcat.1999.2558.

[19] R.Q. Long, R.T. Yang, Catalytic Performance and Characterization of VO^{2+}-Exchanged Titania-Pillared Clays for Selective Catalytic Reduction of Nitric Oxide with Ammonia, J. Catal. 196 (2000) 73–85. doi:10.1006/jcat.2000.3015.

[20] F. Rouquerol, J. Rouquerol, K.S.W. Sing, P. Llewellyn, G. Maurin, Adsorption by powders and porous solids, (2014) 2nd Ed., Elsevier, Oxford, UK, ISBN: 978-0-08-097035-6.

[21] M.D. Alba, M.A. Castro, P. Chain, M.M. Orta, M.C. Pazos, E. Pavón, Hydrothermal stability of layered silicates in neutral and acidic media: Effect on engineered-barrier safety, Clays Clay Miner. 58 (2010) 501–514. doi:10.1346/CCMN.2010.0580405.

[22] M.R. Hoffmann, S.T. Martin, W. Choi, D.W. Bahnemann, Environmental Applications of Semiconductor Photocatalysis, Chem. Rev. 95 (1995) 69–96. doi:10.1021/cr00033a004.

[23] T. Kataoka, J.A. Dumesic, Acidity of unsupported and silica-supported vanadia, molybdena, and titania as studied by pyridine adsorption, J. Catal. 112 (1988) 66–79. doi:10.1016/0021-9517(88)90121-2.

[24] R. Barthos, A study of the acidic and catalytic properties of pure and sulfated zirconia – titania and zirconia – silica mixed oxides, Topics Catal. 10 (2000) 79–87.

[25] F. Lónyi, J. Valyon, J. Engelhardt, F. Mizukami, Characterization and catalytic properties of sulfated ZrO2-TiO2 mixed oxides, J. Catal. 160 (1996) 279–289.

[26] Y.J.Z.Q. Liu Zh, Xing L, Ma H, Cheng L, Liu J, Sulfated Ce-doped TiO_2 as visible light driven photocatalyst: Prepapration, Characterization and Promotin Effects of Ce doping and sulfation on Catalyst PerformanceNo Title, Environ. Prog. Sustain. Energy. 36 (2017) 494–504.

[27] S. Ahmed, M.G. Rasul, W.N. Martens, R. Brown, M.A. Hashib, Heterogeneous photocatalytic degradation of phenols in wastewater: A review on current status and developments, Desalination. 261 (2010) 3–18. doi:10.1016/j.desal.2010.04.062.

[28] J.Á. Pino-Chamorro, T. Ditrói, G. Lente, I. Fábián, A detailed kinetic study of the direct photooxidation of 2,4,6-trichlorophenol, J. Photochem. Photobiol. A Chem. 330 (2016) 71–78. doi:10.1016/j.jphotochem.2016.07.025.

[29] G. Lente, J.H. Espenson, Photoaccelerated oxidation of chlorinated phenols, Chem. Commun. 3 (2003) 1162–1163. doi:10.1039/b301705b.